Acta Cryst. (1997). B53, 135–142

A Re-investigation of the Crystal Structure of the Perovskite $PbZrO_3$ by X-ray and Neutron Diffraction

D. L. CORKER,[a] A. M. GLAZER,[a]* J. DEC,[b] KRYSTIAN ROLEDER[b] AND R. W. WHATMORE[c]

[a]*Department of Physics, Clarendon Laboratory, Parks Road, University of Oxford, Oxford OX1 3PU, England,* [b]*Institute of Physics, Silesian University, Uniwersytecka 4, 40-007, Katowice, Poland, and* [c]*School of Industrial and Manufacturing Science, Cranfield University, Cranfield, Bedfordshire MK43 0AL, England. E-mail: corker@physics.ox.ac.uk*

(Received 26 June 1996; accepted 4 October 1996)

Abstract

The crystal structure of the perovskite lead zirconate $PbZrO_3$ has been redetermined using single-crystal X-ray diffraction (Mo $K\alpha$ radiation, $\lambda = 0.71069$ Å). Single-crystal data at 100 K: space group *Pbam*, $a = 5.884(1)$, $b = 11.787(3)$, $c = 8.231(2)$ Å, $V = 570.85$ Å^3 with $Z = 8$, $\mu = 612.6\,\text{cm}^{-1}$, $D_x = 8.06\,\text{Mg m}^{-3}$, $F(000) = 1168$, final $R = 0.033$, $wR = 0.061$ over 555 reflections with $I > 2\sigma(I)$. An investigation is made into previous contradicting reports of a possible disorder in the oxygens and their origin by examining the crystal pseudo-symmetry. Information distinguishing an ordered and disordered oxygen substructure is shown to reside in weak l odd reflections. Because of their extremely low intensities these reflections have not contributed sufficiently in previous X-ray structure investigations and hence, to date, conclusive evidence differentiating between ordered and disordered models has not been possible. By collecting single-crystal X-ray data at low temperature and by using exceptionally long scans on selected *hkl*, l odd, reflections, a new accurate structure determination is presented and discussed, showing the true ordered oxygen positions. Because of the large difference in scattering factors between lead and oxygen when using X-rays, a neutron diffraction Rietveld refinement using polycrystalline samples (D1A instrument, ILL, $\lambda = 1.90788$ Å) is also reported as further evidence to support the true ordered oxygen structure revealed by the low-temperature X-ray analysis.

1. Introduction

The perovskites of the solid solution series $PbZr_xTi_{1-x}O_3$ have been of considerable interest for many years for their technological applications, resulting from their piezoelectric, ferroelectric and pyroelectric properties. However, throughout this time, achieving accurate structural studies has been severely hampered by various factors, including the inability to prepare single-domain crystals, large numbers of cell doublings, high X-ray absorption, complex structural distortions and pseudo-symmetry. The end compound of this series, $PbZrO_3$, is of particular interest because of its complex temperature phase diagram and the conflicting structural studies published. For many years there has been argument over whether the room-temperature phase of lead zirconate is ferroelectric or antiferroelectric and hence whether the crystal structure belongs to a centrosymmetric or non-centrosymmetric space group. While publications by Roberts (1951) and Dai, Li & Viehland (1995) have reported measurements of weak piezoelectricity and ferroelectricity, similar measurements by Fesenko & Smotrakov (1975) and Scott & Burns (1972) have failed to confirm these observations. Further publications have also indicated a centrosymmetric space group, such as the energetic calculations by Singh (1995) and the convergent-beam electron diffraction measurements of Tanaka, Saito & Tsuzuki (1982).

There have also been conflicting X-ray and neutron diffraction structural investigations, as on two occasions disorder has been reported in the oxygen substructure (Whatmore, 1976; Glazer, Roleder & Dec, 1993), while again in others (Jona, Shirane, Mazzi & Pepinsky, 1957; Fujishita, Shiozaki, Achiwa & Sawaguchi, 1982) no such observation was reported. However, on examination there are differences in the way the investigations took place which exhibited the disorder and those which did not. In those cases where oxygen disorder was seen, the data used came from single-crystal X-ray diffraction experiments, while in powder neutron diffraction studies ordered oxygen positions were reported. In most of the ordered structures reported, the ZrO_6 octahedra tend to be rather distorted, whereas in the disordered structure of Whatmore (1976) and Glazer *et al.* (1993) they were considerably more regular.

This immediately suggests two possibilities: first, the structure of the crystallites in a powder is different from that of a single crystal, a consequence of the different methods of specimen preparation, or second, that the information gained from an X-ray diffraction study is

different from that gained using neutron diffraction. Clearly the most obvious solution to this problem would be to perform an accurate structure solution using single-crystal neutron diffraction data. Unfortunately, no single-domain crystals have yet been grown of sufficient size. Attention was therefore turned towards the details of the disorder and plausible alternative origins of such an apparent disorder.

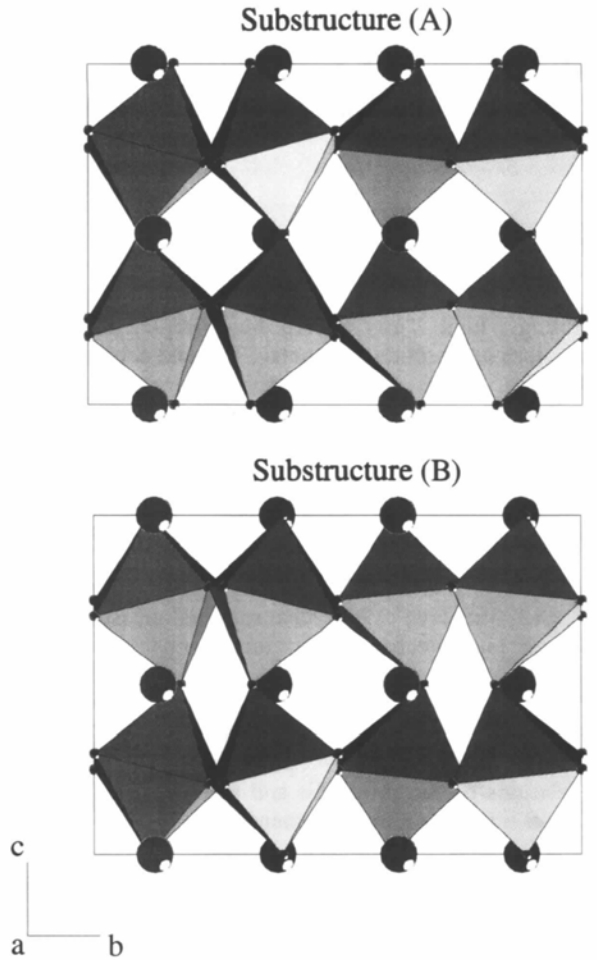

Fig. 1. A model of $PbZrO_3$ showing the possible oxygen substructures (A) and (B).

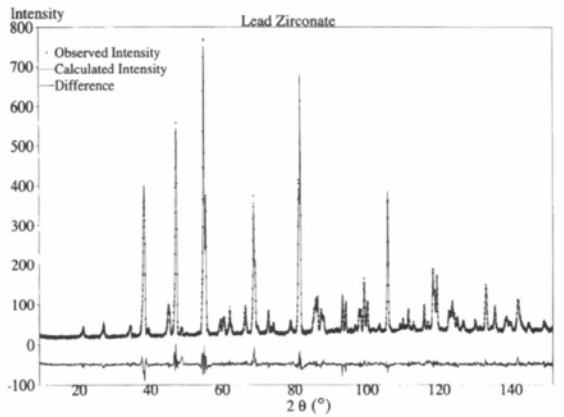

Fig. 2. A comparison of observed and calculated neutron diffraction data for $PbZrO_3$.

In the determination by Glazer *et al.* (1993) the structure was solved in space group *Pbam*, while Whatmore (1976) used space group $P2_12_12$. However, $P2_12_12$ is a subgroup of *Pbam* and in fact both reported disordered structures are actually very similar and can be visualized by the superposition of two oxygen substructures (A) and (B), as shown in Fig. 1. In both reported cases the oxygen coordinates describing these two substructures are approximately related by a translation of $c/2$. One possibility that could explain such an observation is that there exists further cell doublings from the ideal perovskite cell, previously not recognized. However, axial oscillation photographs, each exposed for several days, revealed only the accepted cell doublings originating from the pseudo-cubic perovskite cell (see Fig. 3), namely $4a_p \times 4b_p \times 2c_p$. Incorrect space-group assignment, a common source of split electron density peaks, was also considered. However, use of alternative space groups with the data of Glazer *et al.* (1993) either failed to refine or also exhibited split electron density in calculated Fourier-difference maps, once again indicating a disorder. Another possibility is micro-twinning and although this notion was not initially discarded, this would not explain why the lead and zirconium positions also did not exhibit the apparent disorder.

A similar type of apparent oxygen disorder was found by Sakowski-Cowley, Łukaszewicz & Megaw (1969) in

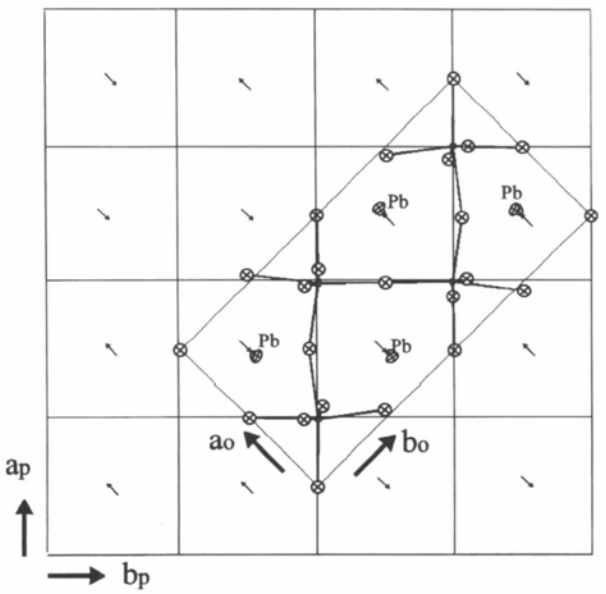

Fig. 3. Pseudo-cubic and conventional orthorhombic unit cells viewed down (001) showing the Pb anti-parallel displacements along a_o.

the perovskite $NaNbO_3$. However, in that case, by forcing one of the oxygens to have full occupancy, the remaining oxygens after refinement became ordered. This did not work in the present case.

A possible solution to this problem can be found when one considers what the reported disorder actually represents. Looking at Fig. 1 we can see that accepting a 50:50 disorder, where the two substructures are related by $c/2$, is equivalent to setting the oxygens in both halves of the unit cell equal. What is possibly lacking, therefore, is sufficient information which can distinguish between the two halves of the unit cell, z: $0 \rightarrow 1/2$ and $1/2 \rightarrow 1$, *i.e.* from the *hkl*, where l = odd, reflections. These reflections, in practice, are extremely weak in comparison to the others.

In space group *Pbam* the Pb-atom positions are on (4*g*) $(x,y,0)$ and (4*h*) $(x,y,\frac{1}{2})$ sites, and the zirconiums on (8*i*) (x,y,z) sites. Since the x,y coordinates of the Pb atoms on the (4*g*) and (4*h*) sites are allowed by symmetry to be different, any small differences between them contribute intensity to the l odd reflections. The zirconiums are also not at special positions and so they too contribute to the l odd reflections. However, both these contributions are small and hence these reflections are heavily dependent on the small deviations of the oxygens from their high-symmetry positions. Given the significantly smaller scattering factor of oxygen in comparison with the cations and the very small departures from high-symmetry sites, we can clearly understand why the l odd reflections are so weak and why it is difficult to separate out the contributions from oxygen and cations. Certainly under normal single-crystal X-ray data collection conditions it would not be surprising if very few, if any, satisfied the usual criteria of acceptance [*e.g.* $I > 3\sigma(I)$] in the data analysis. Even then, those which were accepted would of course be inevitably weighted down by the usual applied weights of $1/\sigma^2(I)$. If a severe lack of these type of reflections were to cause a false disorder it would also be clear why this problem would not occur when using neutron diffraction, as the similar magnitudes of neutron scattering lengths of the oxygens and cations would create much larger l odd reflection intensities.

We made several attempts to overcome these problems by recollecting the X-ray data with l = odd for much longer, but we found it impossible at room temperature to obtain enough data of sufficient quality to enable the separation of the various contributions to be made or to influence the overall refinement of the data.

It was therefore decided that the best solution was to recollect the single-crystal X-ray data, paying particular attention to this problem, and hence to collect data with the emphasis on obtaining a large number of accurate l odd reflections. This would also distinguish between the other possibility of micro-twinning, as examination of the l odd reflections would still indicate a disorder if micro-twinning were present. The methods decided upon to achieve good l odd reflections were:

(i) to collect the data at low temperature to increase general reflection intensities (there is no evidence of a structural phase transition at low temperature in $PbZrO_3$);

(ii) to increase the scan time on all reflections to increase the $I:\sigma(I)$ ratio;

(iii) to select the highest-intensity l odd reflections from this data collection and recollect them using still longer scan times.

2. Synthesis

Lead zirconate crystals were grown from a flux using the system PbO–B_2O_3 as a solvent. A previous polycrystalline preparation of $PbZrO_3$ was taken in the molar proportions 0.77:0.206:0.024 ($PbO:B_2O_3:PbZrO_3$) and soaked in a platinum crucible at 1313 K for 4 h. During crystal growth, a vertical temperature gradient of 10 K cm^{-1} was maintained. The crucible was then cooled at 8 K h^{-1} until a temperature of 1173 K was reached, at which point the solvent was poured out. The crystals were then cooled to room temperature and separated from the crucible by soaking in an aqueous solution of acetic acid. Most crystals had the form of thin, rectangular crystal plates and had a light gray colour. Again, most crystals were also multi-domain. However, very small single-domain crystals of the size 30–40 μm, appropriate for single-crystal X-ray analysis, could most often be found attached to larger 0.5–1 mm multi-domain plates. These could be prised off using quartz fibres, while the large crystal plate was soaked in acetic acid under a polarizing microscope. Simple examination under a polarizing microscope could not distinguish which were suitable for single-crystal X-ray analysis, as many which showed sharp extinction under the microscope were found to possess 90° twinning (such that $a \rightarrow b$ and $b \rightarrow a$) when examined carefully using X-rays. This was visible by the appearance of very weak $\frac{1}{2}kl$ reflections. Therefore, any crystals chosen for single-crystal X-ray data collection were first thoroughly checked for $\frac{1}{2}kl$ reflections using extremely long scans.

A polycrystalline sample of $PbZrO_3$, to be used for powder neutron diffraction, was prepared by the usual ceramic technique of firing mixed oxides of PbO and ZrO_2 powder. PbO (99.999% purity) and ZrO_2 (99.92% purity) were mixed and fired at 1373 K for 12 h. This was followed by a series of grinding and sintering operations until X-ray diffraction showed the expected powder pattern with no impurity lines.

3. X-ray data collection

A single crystal of dimensions 0.02 × 0.03 × 0.06 mm was selected under a polarizing microscope for data

collection on a Stoe Stadi-4 single-crystal diffractometer using Mo $K\alpha$ radiation ($\lambda = 0.71069$ Å) and the ω–2θ scan mode. The crystal was then carefully scanned for $\frac{1}{2}kl$ reflections, as described above, in order to eliminate the possibility of twinning unobserved under the polarizing microscope. The crystal was then cooled to 100 K using an Oxford Cryosystems Cryostream (Cosier & Glazer, 1986) at the rate 70 K h^{-1}. Although the crystal was mounted only by its corner to prevent twinning whilst the adhesive was drying, the $\frac{1}{2}kl$ reflections were scanned again once 100 K was reached in order to monitor possible twinning arising from cooling at this contact. The cell constants were then re-found and refined to the values $a = 5.884(1)$, $b = 11.787(3)$ and $c = 8.231(2)$ Å. Data were then collected over the 2θ range 3–65°, with $-8 < h < 8$, $-17 < k < 17$ and $-12 < l < 12$, while the scan time per reflection was increased to approximately 200 s. During data collection, three standard reflections were monitored every 90 min. Once a full set of data was obtained, 40 of the largest hkl, l odd, reflections were then selected and re-collected using even longer scans (approximately 40 min per reflection). Data reduction was performed using the program *X-RED* (Stoe & Cie, 1994), giving observed systematic absences consistent with space group *Pbam* ($0kl$: $k = 2n + 1$, $h0l$: $h = 2n + 1$, $h00$: $h = 2n + 1$ and $0k0$: $k = 2n + 1$), although the pseudo-symmetric character of the structure meant that many other false sets of absences were apparent, as expected. Data were corrected for absorption using a spherical correction with $\mu r = 1.12$ ($T_{min} = 0.2057$, $T_{max} = 0.2364$).

3.1. *Data analysis and refinement*

Reflections with $I < 2\sigma(I)$ were removed from the data before analysis began using the program *CRYSTALS* (Watkin, Prout, Carruthers & Betteridge, 1996). Initial lead and zirconium positional coordinates were taken from Glazer *et al.* (1993). Oxygen positions were then found from difference-Fourier maps after preliminary refinement of the lead and zirconium positions. At each oxygen site, where in the previous disordered determinations there had been a 50:50 split electron density peak, the site was almost completely dominated by one single peak, although a small residual amount of electron density was still visible at the opposite substructure site. Clearly, although the extra l odd reflections had dramatically improved the situation, the limited number of these reflections still resulted in false electron density (discussed further below). Each main electron density peak did, however, correspond to just one oxygen substructure, namely substructure (B), as represented in Fig. 1. Further refinement of positional and thermal parameters then proceeded without difficulty to an R factor of 0.0326. The refinement was concluded when all shifts were at least two orders of magnitude smaller than the standard deviations in all the parameters. Experimental details are summarized in Table 2. Final atomic positional and thermal parameters are given in Table 3. Zr—O and O—O distances within the ranges 2.04–2.21 and 2.81–3.12 Å, respectively, are listed in Table 4.*

Table 1. *R factors for different models separated into layers of different l*

	Ordered model substructure (B)		Ordered model substructure (A)		Disorder model 50% (A) and 50% (B)	
Layer l	*R*	*wR*	*R*	*wR*	*R*	*wR*
0	0.0375	0.0680	0.0394	0.0726	0.0374	0.0678
1	0.1294	0.1260	0.3415	0.4206	0.2278	0.2428
2	0.0281	0.0471	0.0288	0.0503	0.0281	0.0470
3	0.0973	0.0951	0.3994	0.5040	0.2521	0.2938
4	0.0204	0.0385	0.0200	0.0409	0.0205	0.0384
5	0.1208	0.1143	0.3933	0.4880	0.2523	0.3107
6	0.0255	0.0672	0.0245	0.0678	0.0257	0.0672
7	0.0908	0.0926	0.4386	0.4472	0.2580	0.2854
8	0.0196	0.0320	0.0197	0.0334	0.0197	0.0320
9	0.1086	0.1126	0.4122	0.4736	0.2416	0.2962
10	0.0183	0.0283	0.0231	0.0337	0.0181	0.0281
11	0.0353	0.0390	0.3216	0.4753	0.1761	0.2567
12	0.0502	0.0578	0.0554	0.0666	0.0498	0.0574
	Total $R = 0.0326$		Total $R = 0.0511$		Total $R = 0.0412$	

For comparison purposes the alternative oxygen substructure (A) was then substituted for substructure (B). The R factor immediately rose to 0.0511. Refinement of this substructure was, however, quite impossible, as, although a couple of the oxygens were quite easily trapped in the local minima set up by the small electron density peaks seen earlier in difference-Fourier maps, the remaining oxygens refined immediately back to the opposite substructure (B). The importance of the l odd reflections in distinguishing between these cases is clearly visible when the R factors of the two cases are split into contributions from l odd and l even structure factors. This is shown in Table 1, where the R factors for the models substructure (A) and substructure (B), and a simulated disorder [50% (A) and 50% (B)] are separated into contributions from l: $0 \rightarrow 12$. While the l even contributions are quite consistent throughout the three models, there are considerable differences in the l odd contributions. Note that the contributions from the l odd layers are generally much higher in all cases resulting from their still much smaller $I/\sigma(I)$ ratio in comparison with l even layers. From this examination it is clear that the best fit by far comes from the ordered structure, represented by substructure (B).

Further investigation of the influence of the number of odd reflections used in the analysis was carried out

*Lists of structure factors and the numbered intensity of each measured point on the profile have been deposited with the IUCr (Reference: BM0006). Copies may be obtained through The Managing Editor, International Union of Crystallography, 5 Abbey Square, Chester CH1 2HU, England.

Table 2. *Experimental details*

Crystal data	
Chemical formula	$PbZrO_3$
Chemical formula weight	346.41
Cell setting	Orthorhombic
Space group	*Pbam*
a (Å)	5.884 (1)
b (Å)	11.787 (3)
c (Å)	8.231 (2)
V (Å^3)	570.85
Z	8
D_x (Mg m^{-3})	8.06
Radiation type	Mo $K\alpha$
Wavelength (Å)	0.71069
No. of reflections for cell parameters	51
θ range (°)	9.5–12.5
μ (mm^{-1})	61.26
Temperature (K)	100
Crystal form	Irregular
Crystal size (mm)	0.06 × 0.03 × 0.02
Crystal colour	Grey
Data collection	
Diffractometer	Stoe Stadi-4
Data collection method	ω–2θ scans
Absorption correction	Sphere
T_{min}	0.2057
T_{max}	0.2364
No. of measured reflections	4324
No. of independent reflections	984
No. of observed reflections	555
Criterion for observed reflections	$I > 2\sigma(I)$
R_{int}	0.1335
θ_{max} (°)	32.5
Range of h, k, l	$-8 \rightarrow h \rightarrow 8$ $-17 \rightarrow k \rightarrow 17$ $-12 \rightarrow l \rightarrow 12$
No. of standard reflections	3
Frequency of standard reflections (min)	90
Intensity decay (%)	3
Refinement	
Refinement on	F^2
$R[F^2 > 2\sigma(F^2)]$	0.0326
$wR(F^2)$	0.0607
S	0.996
No. of reflections used in refinement	555
No. of parameters used	28
Weighting scheme	Tukey and Prince weighting scheme with three parameters (10.7, 14.3, 5.0)
$(\Delta/\sigma)_{max}$	0.0001
$\Delta\rho_{max}$ (e Å^{-3})	2.97
$\Delta\rho_{min}$ (e Å^{-3})	−4.15
Extinction method	Larson (1970)
Extinction coefficient	11.5 (4)
Source of atomic scattering factors	*International Tables for X-ray Crystallography* (1974, Vol. IV)

using difference-Fourier maps and refining the true (ordered) oxygen positional and thermal parameters as the $I/\sigma(I)$ threshold was increased. Although this did eliminate a few l even reflections, the weaker l odd reflections were more quickly removed. As soon as the number of l odd reflections decreased several points were noticed. First, the oxygen positional parameters refined closer to the average position of the two alternative substructures. Secondly, both the lead and oxygen temperature factors increased to unreasonably large values. Thirdly, the ratio between electron density

Table 3. *Fractional atomic coordinates and equivalent isotropic displacement parameters (Å^2) from the low-temperature X-ray collection*

$$U_{eq} = (1/3)\Sigma_i\Sigma_j U^{ij} a_i^* a_j^* \mathbf{a}_i.\mathbf{a}_j.$$

	x	y	z	U_{eq}
Pb(1)	0.6991 (1)	0.12988 (5)	0.0	0.0032 (3)
Pb(2)	0.7066 (1)	0.12349 (4)	1/2	0.0045 (3)
Zr(1)	0.2417 (2)	0.1236 (1)	0.2490 (5)	0.0018 (2)
O(1)	0.296 (2)	0.097 (1)	0.0	0.0057 (8)
O(2)	0.278 (2)	0.156 (1)	1/2	0.0057 (8)
O(3)	0.036 (2)	0.2621 (6)	0.220 (1)	0.0057 (8)
O(4)	0.0	1/2	0.297 (2)	0.0057 (8)
O(5)	0.0	0.0	0.270 (2)	0.0057 (8)

Table 4. *Bond lengths (Å) for the oxygens in the octahedra*

Zr(1)—O(1)	2.098 (5)	O(1)—O(3)	3.07 (1)
Zr(1)—O(2)	2.111 (5)	O(2)—O(4^i)	2.81 (1)
Zr(1)—O(3)	2.047 (8)	O(2)—O(3^i)	2.92 (1)
Zr(1)—O(3^i)	2.205 (8)	O(2)—O(3)	2.98 (1)
Zr(1)—O(4^i)	2.142 (3)	O(2)—O(5)	3.10 (1)
Zr(1)—O(5)	2.044 (2)	O(3)—O(3^i)	2.96 (1)
O(1)—O(3^i)	2.84 (1)	O(3)—O(5)	3.123 (8)
O(1)—O(4^i)	2.95 (1)	O(3^i)—O(4^i)	2.881 (8)
O(1)—O(5)	3.05 (1)	O(4^i)—O(5)	2.95 (1)

Symmetry code: (i) $\frac{1}{2} + x, \frac{1}{2} - y, z$.

visible at the two alternative substructure sites decreased. Although the present refinement gives sensible temperature factors, concern had to be given to whether the positional parameters were still weighted to converging towards the substructure (A) 'ghost'. It was therefore decided as a check on this possibility by redetermining the oxygen positional parameters from powder neutron diffraction for comparison.

4. Neutron data collection and Rietveld analysis

Neutron powder diffraction data were collected at 398 K using the diffractometer D1A at the Institut Max Von Laue–Paul Langevin (Grenoble, France). The choice of high temperature at which the data were collected was simply due to experimental practicalities, as limited experimental time prevented a total cool down to room temperature after a previous high-temperature phase experiment. However, as the material undergoes a transition from its room-temperature phase to its paraelectric phase at around 503 K, it was felt that the material was sufficiently far from its transition for relevant data to be collected.

The $PbZrO_3$ sample was held in a cylindrical vanadium holder (height 6 cm, diameter 1 cm), while data were collected to $\theta_{max} = 79.48°$, with 0.025° steps, and $\lambda = 1.90788$ Å. The program *FULLPROF* (Rodriguez-Carvajal, 1995) was used for Rietveld refinement with the neutron elastic scattering lengths $b_{Pb} = 9.405$, $b_{Zr} = 7.160$, $b_O = 5.803$ fm. The background was refined using a polynominal function, while

Table 5. *Fractional atomic coordinates and equivalent isotropic displacement parameters ($Å^2$) from the neutron Rietveld refinement of $PbZrO_3$ at 398 K*

$U_{eq} = (1/3)\sum_i\sum_j U^{ij} a_i^* a_j^* \mathbf{a}_i.\mathbf{a}_j.$

	x	y	z	U_{eq}
Pb(1)	0.717 (1)	0.1311 (5)	0.0	0.022 (3)
Pb(2)	0.707 (1)	0.1269 (5)	1/2	0.024 (3)
Zr(1)	0.2438 (4	0.1236 (5)	0.251 (1)	0.007 (2)
O(1)	0.292 (2)	0.0988 (9)	0.0	0.017 (2)
O(2)	0.271 (2)	0.1516 (9)	1/2	0.015 (2)
O(3)	0.025 (1)	0.2597 (3)	0.2269 (7)	0.013 (2)
O(4)	0.0	1/2	0.2925 (8)	0.020 (2)
O(5)	0.0	0.0	0.273 (1)	0.021 (2)

the peak shapes were described by a pseudo-Voigt profile.

Although X-ray powder diffraction patterns, simulated using the program *Crystallographica* (Oxford Cryosystems, 1996), for the ordered and disordered models taken from Glazer *et al.* (1993) were indistinguishable from each other, the simulated neutron powder diffraction profiles for the two models did show significant differences, especially in the l odd reflections. In particular, with neutrons, the ordered model gave an approximate tenfold increase in intensities of the 141, 221 and 023 reflections over those of the disordered model. As these reflections were clearly visible in the experimentally observed pattern (023 being around 8% of the maximum intensity), it was therefore clear that the observed pattern represented the ordered structure.

The initial atomic coordinates were therefore taken from the present X-ray data analysis, although other models were later inserted to prevent positional parameters converging to false minima. Lead and zirconium were refined anisotropically, while the oxygens had to be kept isotropic because of the otherwise poor parameter-to-reflection ratio. The R factor converged quickly to the values $R_p = 0.118$ with $\chi^2 = 1.97\%$. Fig. 2 shows the observed, calculated and difference neutron diffraction profiles.* Final positional and thermal parameters are given in Table 5, while the oxygen positions found by Glazer *et al.* (1993) are given in Table 6 for comparison. Further experimental details are summarized in Table 7.

Again, refinement of the opposite oxygen substructure was attempted. However, this either resulted in immediate convergence back to the first substructure; or if the refinement was restricted to hold the second substructure in place, the oxygen temperature factors increased to unreasonably high values. The lowest obtainable R factor with this technique was 0.13.

*The diffraction peak seen at approximately $2\theta = 48.7°$ in the observed diffraction pattern is not observed in the calculated pattern as it originates from the furnace in which it was placed. In order that this did not affect the refined parameters the profile in the 2θ range 48.0–49.2° was removed from the calculations.

Table 6. *Oxygen fractional coordinates for substructures (A) and (B) in the disordered model obtained by Glazer et al. (1993)*

Glazer *et al.* (1993)
Room temperature

		x	y	z
O(1)	(A)	0.3083	0.1720	0.0
	(B)	0.3057	0.1132	
O(2)	(A)	0.2993	0.1044	1/2
	(B)	0.3103	0.1770	
O(3)	(A)	0.0316	0.2666	0.2914
	(B)	0.0292	0.2651	0.2089
O(4)	(A)	0.0	1/2	0.1993
	(B)	0.0	1/2	0.2980
O(5)	(A)	0.0	0.0	0.2507

Table 7. *Neutron experimental details*

Crystal data	
Chemical formula	$PbZrO_3$
Chemical formula weight	346.41
Cell setting	Orthorhombic
Space group	*Pbam*
a (Å)	5.8878 (2)
b (Å)	11.7890 (4)
c (Å)	8.2527 (2)
V ($Å^3$)	572.83
Z	8
D_x (Mg m^{-3})	8.03
Radiation type	Neutron
Wavelength (Å)	1.90788
θ range (°)	0–79.48
μ (mm^{-1})	0.001
Temperature (K)	398
Data collection	
Diffractometer	D1A, ILL
Monochromator	Germanium
2θ step (°)	0.05
Sample container	Vanadium holder
Instrument geometry	25 ^{3}He detectors
θ_{max} (°)	79.48
Refinement	
Refinement on	Polynomial function
R (LS/conventional)	0.0575/0.118
wR (LS/conventional)	0.07681/0.129
R_{exp} (LS/conventional)	0.0547/0.0918
$R_I = \Sigma(I_i - I_{ci})/\Sigma I_i$	0.0467
No. of parameters used	51
χ^2	1.97
FWHM	$u\tan^2\theta + v\tan\theta + w$
Weighting scheme	$w = 1/\sigma^2(I)$
$(\Delta/\sigma)_{max}$	0.1
Analytical function for profile	Pseudo-Voigt
Computer programs	
Structure refinement	*FULLPROF* (Rodriguez-Carvajal, 1995)
Molecular graphics	*Crystallographica* (Oxford Cryosystems, 1996)

From Tables 5 and 6 it can be immediately observed that the coordinates of the present work correspond to those of substructure (B) given by Glazer *et al.* (1993), while comparison of Tables 3 and 5 shows the oxygen coordinates obtained in the present powder neutron and low-temperature single-crystal X-ray diffraction studies are very close, especially considering the large

temperature difference at which the experiments had been carried out. We can therefore assume that the number of l odd reflections used in the low-temperature single-crystal X-ray analysis was sufficient for the oxygen positional parameters to converge at least very close to their true positions rather than, as feared, biased towards the opposite 'ghost' substructure, a problem which is apparent in many of the oxygen parameters given by Glazer *et al.* (1993).

5. Detecting centrosymmetry

As previously discussed, not only has there been controversy over the presence of oxygen disorder, but also as to whether the material is ferroelectric or antiferroelectric. In crystallographic terms this depends on whether the crystal symmetry contains an inversion or not and hence on whether the point group is polar or non-polar. If the true symmetry were non-centrosymmetric then the space group would be *Pba*2 (or of lower symmetry still) rather than, as described above, *Pbam*. However, many attempts at structure solution using the space group *Pba*2 proved fruitless. Even when harsh restrictions were imposed to prevent the refinement from 'exploding' because of high correlation between parameters, the outcome was either physically unlikely or deviated negligibly from its centrosymmetric equivalent. However, as the true deviations from the *Pbam* model could be smaller than those consistent with the sensitivity of the X-ray data, it was thought worthwhile to attempt to measure a polar-sensitive physical property. The chosen measurement sensitive to a centre of symmetry was second-harmonic generation (SHG).

The experimental set-up used to detect any second-harmonic signal was based on the apparatus described by Kurtz & Perry (1968). A powdered sample of $PbZrO_3$ was placed in an intense beam from a Q-switched Nd:YAG laser of wavelength 1064 nm. The output, first filtered to remove the fundamental beam, was then detected using a photomultiplier. Apart from a small, initially registered signal which quickly decayed with time, a common occurrence with lead compounds independent of whether they are centrosymmetric or non-centrosymmetric, no positive second-harmonic signal (532 nm) could be detected to within the accuracy provided by the apparatus.

A negative observation of second-harmonic generation unfortunately does not prove the material is centrosymmetric and hence truly antiferroelectric. However, it does justify continuing to assume the structure has a centre of symmetry until future opposing evidence is reported.

6. Results

To within the accuracy of the X-ray structure analysis and SHG measurements performed thus far, the indications are that the room-temperature phase of lead zirconate is antiferroelectric, space group *Pbam*, with the Pb atoms showing anti-parallel shifts from the high-symmetry perovskite positions described in Fig. 3. As indicated in this figure, the greatest anti-parallel shifts are along [100]. The low-temperature X-ray analysis gives these as approximately 0.30 Å for Pb(1) and 0.26 Å for Pb(2), although much smaller shifts, 0.06 and 0.02 Å for Pb(1) and Pb(2), respectively, are also visible along [010]. These shifts are greater than those reported in previous structural investigations on lead zirconate, because the present X-ray investigation was carried out at low (100 K) temperature and hence further away from its high-temperature cubic perovskite phase. Lead zirconate undergoes its paraelectric–antiferroelectric phase transition around 503 K. The reduction in anti-parallel shift of the Pb x coordinate as the temperature is increased towards the phase transition can be seen by comparing the average Pb shift in the present X-ray analysis, the room-temperature determination by Glazer *et al.* (1993) and those obtained in the present neutron powder profile refinement carried out at a relatively high temperature of 398 K (Table 8). The behaviour of these shifts, although far from the transition, is clearly visible. However, further investigation into the structural changes as the transition is closely approached is under way and will be published in the near future.

Table 8. *Showing the gradual decrease in anti-parallel Pb shifts with increasing temperature*

Report	Temperature (K)	Average Pb [100] shift (Å)
Present X-ray single-crystal diffraction analysis	100	0.28
Glazer *et al.* (1993)	293	0.25
Present neutron powder diffraction analysis	398	0.22

By placing the emphasis on the measurement of l odd reflections in the X-ray single-crystal data collection, oxygen coordinates have been located with new precision. Previous reports of a disorder have been shown to be the result of an artifact originating from pseudo-symmetry and the comparatively small scattering factor of oxygen. Although neutron Rietveld refinement was used as a simple check on the oxygen displacements, the fact that a thorough structure analysis was carried out using pure single-crystal data probably eliminates the possibility of a difference between the structure of crystallites in the powder and that of a single crystal. It is true to say that there still remains a possibility that there could be a change in oxygen ordering/disordering in the single crystal in going from room to low temperature; however, this is a most unlikely prospect, as there is no supporting physical evidence for such a phenomenon. Inclusion of l odd reflections into the single-crystal analysis also

gave the refinement the sensitivity to observe that there is a definite, although small [approximately 0.008(4) Å], departure of the Zr atom from the $z = 0.25$, 0.75 planes, a feature not previously visible in earlier lead zirconate structure determinations.*

The authors would like to thank the Institut Max von Laue-Paul Langevin (ILL), Grenoble, France, for enabling the neutron diffraction experiment to be carried out. We would also like to express our gratitude towards Dr Francois Fauth for his assistance during our time at the ILL and for his continuing support and advice. We also thank the Engineering and Physical Sciences Research Council (EPSRC) for providing the grant for this investigation.

* Although a recent abstract to the IUCr XVII Congress and General Assembly at Seattle, USA (Yamasaki, K., Soejima, Y. & Fischer, K. F., 1996), also supports an anti-phase displacement of Zr along [001].

References

Cosier, J. & Glazer, A. M. (1986). *J. Appl. Cryst.* **19**, 105–107.

Dai, X., Li, J. F. & Viehland, D. (1995). *Phys. Rev. B*, **51**, 2651.

Fesenko, O. E. & Smotrakov, V. G. (1975). *Ferroelectrics*, **12**, 211–213.

Fujishita, H., Shiozaki, Y., Achiwa, N. & Sawaguchi, E. (1982). *J. Phys. Soc. Jpn*, **51**, 3583–3591.

Glazer, A. M., Roleder, K. & Dec, J. (1993). *Acta Cryst.* B**49**, 846–852.

Jona, F., Shirane, G., Mazzi, F. & Pepinsky, R. (1957). *Phys. Rev.* **105**, 849–856.

Kurtz, S. K. & Perry, T. T. (1968). *J. Appl. Phys.* **39**, 3798–3813.

Oxford Cryosystems (1996). *Crystallographica. A Crystallographic Data Software Tool*. Oxford Cryosystems, Long Hanborough, England.

Roberts, S. (1951). *Phys. Rev.* **83**, 1078.

Rodriguez-Carvajal, J. (1995). *FULLPROF. A Rietveld Refinement and Pattern Matching Analysis Program*. Laboratoire Leon Brillouin (CEA-CNRS), France.

Sakowski-Cowley, A. C., Łukaszewicz, K. & Megaw, H. D. (1969). *Acta Cryst.* B**25**, 851–865.

Scott, B. A. & Burns, G. (1972). *J. Am. Ceram. Soc.* **55**, 331.

Singh, D. J. (1995). *Phys. Rev. B*, **52**, 12559–12563.

Stoe & Cie (1994). *X-RED. Data Reduction Program. STADI4. Data Collection Program*. Stoe & Cie, Darmstadt, Germany.

Tanaka, M., Saito, R. & Tsuzuki, K. (1982). *J. Phys. Soc. Jpn*, **51**, 2635–2640.

Watkin, D. J., Prout, C. K., Carruthers, J. R. & Betteridge, P. W. (1996). *CRYSTALS*, Issue 10. Chemical Crystallography Laboratory, University of Oxford.

Whatmore, R. W. (1976). D.Phil. Thesis. Cavendish Laboratory, Cambridge, England.